2932 *Biochemistry* **2010,** *49,* 2932–2942
DOI: 10.1021/bi100159p

BIOCHEMISTRY
including biophysical chemistry & molecular biology
Article

Characterization of the Colchicine Binding Site on Avian Tubulin Isotype βVI[†]

Shubhada Sharma,[‡] Barbara Poliks,[§] Colby Chiauzzi,[§] Rudravajhala Ravindra,[‡] Adam R. Blanden,[‡] and Susan Bane*,[‡]

[‡]*Department of Chemistry, Binghamton University, State University of New York, Binghamton, New York 13902, and* [§]*Department of Physics, Binghamton University, State University of New York, Binghamton, New York 13902*

Received February 1, 2010; Revised Manuscript Received February 22, 2010

ABSTRACT: Tubulin, the basic component of microtubules, is present in most eukaryotic cells as multiple gene products, called isotypes. The major tubulin isotypes are highly conserved in terms of structure and drug binding capabilities. Tubulin isotype βVI, however, is significantly divergent from the other isotypes in sequence, assembly properties, and function. It is the major β-tubulin isotype of hematopoietic tissue and forms the microtubules of platelet marginal bands. The interaction of the major tubulin isotypes βI, βII, βIII, and βIV with antimicrotubule drugs has been widely studied, but little is known about the drug binding properties of tubulin isotype βVI. In this investigation, we characterize the activity of various colchicine site ligands with tubulin isolated from *Gallus gallus* erythrocytes (CeTb), which is ∼95% βVI. Colchicine binding is thought to be a universal property of higher eukaryotic tubulin; however, we were unable to detect colchicine binding to CeTb under any experimental conditions. Podophyllotoxin and nocodazole, other colchicine site ligands with divergent structures, were able to inhibit paclitaxel-induced CeTb assembly. Surprisingly, the colchicine isomer allocolchicine also inhibited CeTb assembly and displayed measurable, moderate affinity for CeTb ($K_a = 0.18 \times 10^5$ M^{-1} vs 5.0×10^5 M^{-1} for bovine brain tubulin). Since allocolchicine and colchicine differ in their C ring structures, the two C ring colchicine analogues were also tested for CeTb binding. Kinetic experiments indicate that thiocolchicine and chlorocolchicine bind to CeTb, but very slowly and with low affinity. Molecular modeling of CeTb identified five divergent amino acid residues within 6 Å of the colchicine binding site compared to βI, βII, and βIV; three of these amino acids are also altered in βIII-tubulin. Interestingly, the altered amino acids are in the vicinity of the A ring region of the colchicine binding site rather than the C ring region. We propose that the amino acid differences in the binding site constrict the A ring binding domain in CeTb, which interferes with the positioning of the trimethoxyphenyl A ring and prevents C ring binding site interactions from efficiently occurring. Allocolchicine is able to accommodate the altered binding mode because of its smaller ring size and more flexible C ring substituents. The sequence of the colchicine binding domain of CeTb isotype βVI is almost identical to that of its human hematopoietic counterpart. Thus, through analysis of the interactions of ligands with CeTb, it may be possible to discover colchicine site ligands that specifically target tubulin in human hematopoietic cells.

Microtubules are the targets for a wide variety of substances whose utility ranges from herbicides and fungicides to anticancer drugs (*1*−*3*). The vast majority of these molecules act by binding to the protein tubulin, an α,β-heterodimer that forms the core of the microtubule. Tubulin is a highly conserved and ubiquitous protein, typically containing only 2−8% amino acid sequence divergence and found in every eukaryotic cell. Organisms possess multiple genes for each tubulin subunit, which are termed isotypes (*4*). Each tubulin isotype is also subject to posttranslational modifications, so the microheterogeneity of tubulin within a single cell can be enormous (*5*). Although this is true for both α- and β-tubulin, much more is known about β-isotypes because they contain the binding sites of clinically relevant drugs (*6*). The mammalian and avian β-isotypes have been classified into seven categories (*5*). Some of these isotypes, such as βI and βIVb, are distributed widely among different tissues (*7*). Others seem to be restricted to specific organs and cells. Particular interest has been paid to isotype βIII, which is normally found in specific cells in the brain, testis, and colon. Overexpression of this isotype in several types of cancer cells has been correlated with paclitaxel resistance and poor prognosis (*7*−*11*).

Although tubulin exists in multiple isotypes, its drug binding properties with respect to the antimitotic agent colchicine are almost universally conserved among higher-order eukaryotes (*12*). The affinity of the protein for colchicine decreases in lower-order eukaryotes, but even tubulin from yeast such as *Saccharomyces cerevisiae* weakly binds colchicine (*13*). Tubulin from bovine brain (BbTb),[1] a common source of purified tubulin, is composed of β-tubulin isotypes βI, βII, βIII, and βIV in relative amounts of 3, 58, 25, and 13%, respectively (*4*). Studies with mammalian brain tubulin have established that colchicine binding to

[†]Financial support was provided by the National Institutes Health (Grant CA-69571).

*To whom correspondence should be addressed. Phone: (607) 777-2927. Fax: (607) 777-4478. E-mail: sbane@binghamton.edu.

[1]Abbreviations: BbTb, bovine brain tubulin; CeTb, chicken erythrocyte tubulin; DEAE, diethylaminoethylcellulose; DMSO, dimethyl sulfoxide; EGTA, ethylene glycol bis(2-aminoethyl ether)-*N*,*N*,*N*′,*N*′-tetraacetic acid; G-50, Sephadex G-50; GTP, guanosine 5′-triphosphate; MAPs, microtubule-associated proteins; $MgSO_4$, magnesium sulfate; PIPES, piperazine 1,4-bis(2-ethanesulfonic acid); PME, 0.1 M PIPES, 1 mM $MgSO_4$, and 2 mM EGTA at pH 6.90 and 25 °C.

 Published on Web 02/23/2010

tubulin is slow, highly temperature dependent, and effectively irreversible. The binding is accompanied by conformational changes in the protein and unique alterations in optical spectra of colchicine (*14*). Intraspecies differences in colchicine binding properties of tubulin were first detected by kinetic studies. Biphasic curves corresponding to parallel reactions were observed for the association of colchicine with BbTb (*15*). Ludueña and co-workers demonstrated that the minor phase of the association kinetics reaction is due to colchicine binding to isotype βIII of bovine brain tubulin (*16*). Subsequent drug binding measurements performed on purified isotypes demonstrated that all of the β-tubulin isotypes investigated have a slightly different affinity for colchicine and other colchicine site ligands. The differences in affinity, however, are relatively small for most ligands, the difference in association constants normally varying from a factor of 2 to a factor of 10 (*17*−*21*).

The major β-tubulin isotype in hematopoietic tissue, βVI, resists the observation that the primary sequence is conserved within higher-order eukaryotes (*22*). Termed β1-tubulin when derived from mouse or human, it forms the marginal band in platelets, and its sequence divergence is thought to reflect its specialized structural role in these cells. Chick βVI-tubulin can co-assemble in vivo into microtubules in mammalian cells (*23*), but β1-tubulin knockout mice have thrombocytopenia and defective marginal bands (*24*). Of the seven β-tubulin categories, isotype βVI has the most diverse primary sequence. For example, avian βVI exhibits overall 17% divergence in its amino acid sequence compared with other avian β-tubulins. It is more hydrophobic, containing seven fewer net negative charges, and assembles in vitro more efficiently but with a nucleation rate lower than that of brain tubulin (*22*, *25*). Additionally, it assembles into microtubules that are longer than that those composed of brain tubulin (*26*). The conspicuous divergence of isotype βVI from all other β-isotypes prompts the study of its interaction with colchicine site drugs that bind well to brain tubulin. Chicken erythrocytes were chosen as the tubulin source, since avian erythrocyte tubulin is ~95% βVI and the assembly properties of the pure protein have been studied well (*27*, *28*).

In this work, we investigate the effect of avian βVI sequence divergence on the colchicine binding site and drug binding properties thereof compared to those of mammalian brain tubulin. The ligands explored were colchicine, allocolchicine, podophyllotoxin, chlorocolchicine, thiocolchicine, and nocodozole (Figure 1), all of which are known to bind BbTb at the colchicine site. The results of these studies are discussed in light of sequence differences within the colchicine binding site of β-tubulin isotypes.

MATERIALS AND METHODS

Chemicals used were analytical grade and purchased from Sigma-Aldrich. All experiments with tubulin were performed in PME (100 mM Pipes, 1 mM $MgSO_4$, and 2 mM EGTA at pH 6.90 and 25 °C) with freshly added 0.1 mM GTP. Spectrograde solvents were used in absorption and fluorescence spectroscopy. Allocolchicine, thiocolchicine, and chlorocolchicine were synthesized in our lab (*29*). All colchicinoids and allocolchicine were pure as determined by thin layer chromatography, and their structures were confirmed by proton NMR spectroscopy and mass spectrometry.

Stock solutions of paclitaxel, podophyllotoxin, nocodazole, allocolchicine, chlorocolchicine, and thiocolchicine were made in DMSO. Colchicine stock solutions were made in water or in

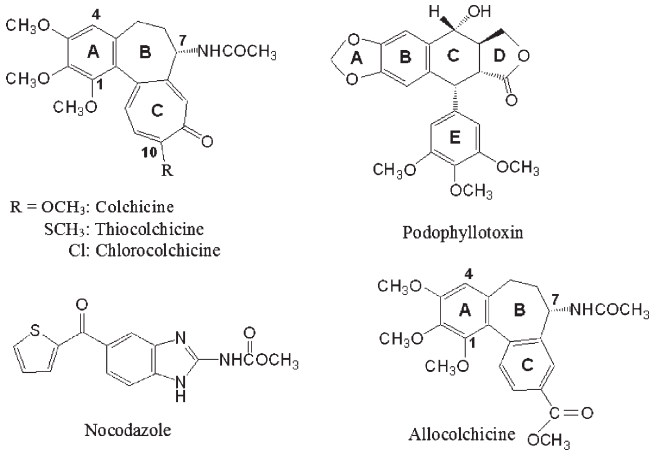

FIGURE 1: Structures of colchicine, chlorocolchicine, thiocolchicine, podophyllotoxin, nocodazole, and allocolchicine.

buffer. Ligand concentrations were determined spectrophotometrically using the following extinction coefficients: $\varepsilon_{273\ DMSO} = 0.17 \times 10^4\ M^{-1}\ cm^{-1}$ for paclitaxel, $\varepsilon_{353\ water} = 1.7 \times 10^4\ M^{-1}\ cm^{-1}$ for colchicine (*30*), $\varepsilon_{295\ DMSO} = 1.8 \times 10^4\ M^{-1}\ cm^{-1}$ for allocolchicine, $\varepsilon_{324\ DMSO} = 1.4 \times 10^4\ M^{-1}\ cm^{-1}$ for nocodazole, $\varepsilon_{294\ DMSO} = 0.45 \times 10^4\ M^{-1}\ cm^{-1}$ for podophyllotoxin (*31*), $\varepsilon_{353\ DMSO} = 0.97 \times 10^4\ M^{-1}\ cm^{-1}$ for chlorocolchicine, and $\varepsilon_{380\ DMSO} = 1.6 \times 10^4\ M^{-1}\ cm^{-1}$ for thiocolchicine (*29*).

Tubulin Purification. BbTb was prepared by two cycles of temperature-dependent assembly and disassembly as described by Williams and Lee (*32*). The protein solution from the end of the second cycle was subjected to ion exchange chromatography on phosphocellulose resin to yield purified tubulin.

Chicken erythrocyte tubulin (CeTb) was isolated from whole blood purchased from Pel-Freez Biologicals (Rogers, AR) using a procedure adapted from Sackett (*33*). Briefly, the erythrocytes were pelleted at 2500*g* for 10 min at 4 °C and washed with 0.9% saline. The pellet was resuspended in 0.6 volume of PMCG (100 mM PIPES, 1 mM $MgCl_2$, 2 mM $CaCl_2$, and 0.1 mM GTP). The suspension was sonicated at 4 °C to disrupt the cells and centrifuged at 10000*g* at the same temperature for 30 min. The supernatant was incubated with DE52 chromatography resin previously equilibrated with PME. The resin was washed with PME to remove hemoglobin and centrifuged at 1250 rpm in an IEC Centra-7R refrigerated centrifuge at 4 °C for 1 min to pellet the resin. This was followed by three washings and centrifugations with PMCG buffer supplemented with 0.25 M glutamate buffer. Finally, tubulin was eluted using 0.75 M glutamate in PMCG buffer. The CeTb was pure as determined by SDS−PAGE.

The MAP-free BbTb and CeTb were drop-frozen in liquid nitrogen. Prior to use, the frozen pellets were gently thawed and then desalted into PME buffer by the method of Penefsky (*34*). The concentration of BbTb or CeTb was determined spectrophotometrically using an extinction coefficient of $1.23\ M^{-1}\ cm^{-1}$ at 278 nm in PME (*35*).

IC_{50} Determination. The IC_{50} of the assembly inhibiting agent is defined as the total concentration of inhibitor required to reduce the extent of tubulin polymerization by 50% of its value in the absence of added inhibitor. The procedure was as follows. BbTb or CeTb (5 μM) in PME was incubated with varying concentrations of colchicine, podophyllotoxin, or nocodazole at 25 °C for 90, 25, or 40 min, respectively, in the presence of 0.1 mM GTP. The incubated protein samples were equilibrated to 37 °C in the sample cells of a Hewlett-Packard 8453 UV−vis

spectrophotometer with a thermostated multicell holder, and a baseline was recorded. Paclitaxel in DMSO was added to a concentration of 5 μM to initiate polymerization. The final concentration of DMSO was kept at 2% (v/v). The extent of polymerization was assessed as the plateau value of apparent absorption at 400 nm for colchicine and podophyllotoxin and 350 nm for other ligands. The IC_{50} values were calculated from nonlinear regression fits of sigmoidal plots of percent polymerization versus ligand concentration using SigmaPlot version 10.0 (Systat Software Inc., San Jose, CA).

Fluorescence Spectroscopy. All fluorescence measurements were performed in a Jobin Yvon Fluorolog 3 spectrofluorometer in a thermostated cell. A 2 mm × 10 mm fluorescence cell was oriented such that the excitation beam passed through the shorter path length, and the temperature was maintained at 25 °C using a circulating water bath.

Measurement of Association Kinetics. (*i*) *Colchicine*. The kinetics of colchicine binding to tubulin were monitored by the increase in colchicine fluorescence or the decrease in intrinsic protein fluorescence as a function of time. Experiments monitoring fluorescence enhancement of colchicine in the presence of CeTb or BbTb were conducted as follows. A solution of colchicine (150 μM) in PME containing 0.1 mM GTP was equilibrated in the fluorescence cell in the spectrofluorometer. Tubulin was added to a final concentration of 1 μM. The sample was rapidly mixed, and the shutters were opened to monitor the fluorescence. The excitation and emission wavelengths were 340 and 440 nm, respectively. The kinetics of intrinsic fluorescence quenching of tubulin in the presence of colchicine were measured as described above except that colchicine was added to a preequilibrated tubulin solution and the excitation and emission wavelengths were 295 and 335 nm, respectively.

(*ii*) *Allocolchicine*. The association of allocolchicine with tubulin as a function of time was observed by monitoring the increase in allocolchicine fluorescence that accompanies tubulin binding (*36*). All measurements of allocolchicine association kinetics were performed under the same conditions that were used for colchicine fluorescence enhancement kinetics except that 10% DMSO was included in the samples to ensure the solubility of the ligand. The excitation and emission wavelengths were 330 and 400 nm, respectively.

(*iii*) *Thiocolchicine and Chlorocolchicine*. The kinetics of thiocolchicine or chlorocolchicine binding to tubulin were assessed by recording the decrease in tubulin fluorescence as a function of time, with excitation and emission wavelengths of 295 and 335 nm, respectively. The experiments with CeTb were performed in the same manner described for colchicine except that DMSO (10%, v/v) was included in the samples to promote the solubility of ligands. Kinetics of ligand binding to BbTb were measured using 20 μM ligand because the chlorocolchicine reaction occurred too quickly at the higher concentration to accurately measure on the spectrofluorometer. The apparent second-order rate constants for the colchicinoids binding to BbTb were comparable with those measured previously (*30*, *37*).

Kinetic Data Analysis. The data of increasing ligand fluorescence or decreasing protein fluorescence as a function of time were fit to a double exponential for BbTb:

$$F_t = Ae^{-\alpha t} + Be^{-\beta t} + C$$

where F_t is the fluorescence at time t, α and β are the observed pseudo-first-order rate constants of the fast and slow phases, respectively, A and B are the amplitudes of these two phases, and C is an integration constant. When the data were from increasing fluorescence intensity, F_t was the observed fluorescence intensity at each time interval after subtraction of the initial fluorescence value. For data of decreasing fluorescence intensity, F_t was defined as the absolute value of the fluorescence at time zero minus the fluorescence value at each time interval. The parameters A, B, α, and β were obtained by nonlinear curve fitting software from SigmaPlot version 10.0. The apparent second-order rate constant for the fast phase for each ligand ($k_{on,app}$) was calculated as α/c, where c is the total concentration of the ligand.

The fluorescence data as a function of time for ligand binding to CeTb were fit to a single exponential

$$F_t = Ae^{-\alpha t} + C$$

where F_t is the fluorescence at time t, defined in the same manner as for the BbTb experiments, α is the observed pseudo-first-order rate constant, A is the amplitude, and C is an integration constant. The data were fit using SigmaPlot, and the apparent second-order rate constants for each ligand were calculated as described above.

Equilibrium Measurements of the Association of Allocolchicine with Tubulin. The constant for association of allocolchicine for BbTb or CeTb at 25 °C was determined by fluorescence titration. Samples of BbTb or CeTb (1 μM) in PME and 0.1 mM GTP were incubated with varying concentrations of allocolchicine at 25 °C for 90 min. The samples were excited at 315 nm, and the emission intensity at 400 nm was measured. The final DMSO concentration was maintained at 10%. Blank spectra of the buffer without fluorophore were recorded and subtracted to correct for background fluorescence.

The emission intensity of allocolchicine was corrected for inner filter effects as described by Lakowicz (*38*) using the equation

$$F_{corr} = F_{obs}\,\text{antilog}[(A_{ex} + A_{em})/2]$$

where F_{obs} is the observed emission intensity of allocolchicine, F_{corr} is the emission intensity corrected for the inner filter effect, and A_{ex} and A_{em} are the absorbances of allocolchicine at the excitation (315 nm) and emission (400 nm) wavelengths, respectively. A_{ex} was divided by 5 before being applied to the equation, to account for the shorter path of the excitation beam.

The corrected data were then analyzed according to the following equation (*36*):

$$\alpha/[\text{allo}]_{free} = -K\alpha + nK$$

where α is the fraction of tubulin bound, or [complex]/To, where To is the total tubulin concentration, $[\text{allo}]_{free}$ is the concentration of the unbound ligand (calculated as $[\text{allo}]_{free} = [\text{allo}]_0 - \alpha\text{To}$, where $[\text{allo}]_0$ is the total allocolchicine concentration), n (number of binding sites) equals 1, and K is the association constant.

The fraction of tubulin bound (α) was determined by

$$\alpha = F/F_{max}$$

where F_{max} is the fluorescence intensity at a saturating concentration of allocolchicine and F is the fluorescence measured at any allocolchicine concentration.

Inhibition of Allocolchicine Binding to Tubulin by Podophyllotoxin. Podophyllotoxin inhibits the binding of allocolchicine to tubulin by blocking the binding site (*39*). To confirm the binding of podophyllotoxin as well as allocolchicine to CeTb at the same discrete binding site, we compared the binding of

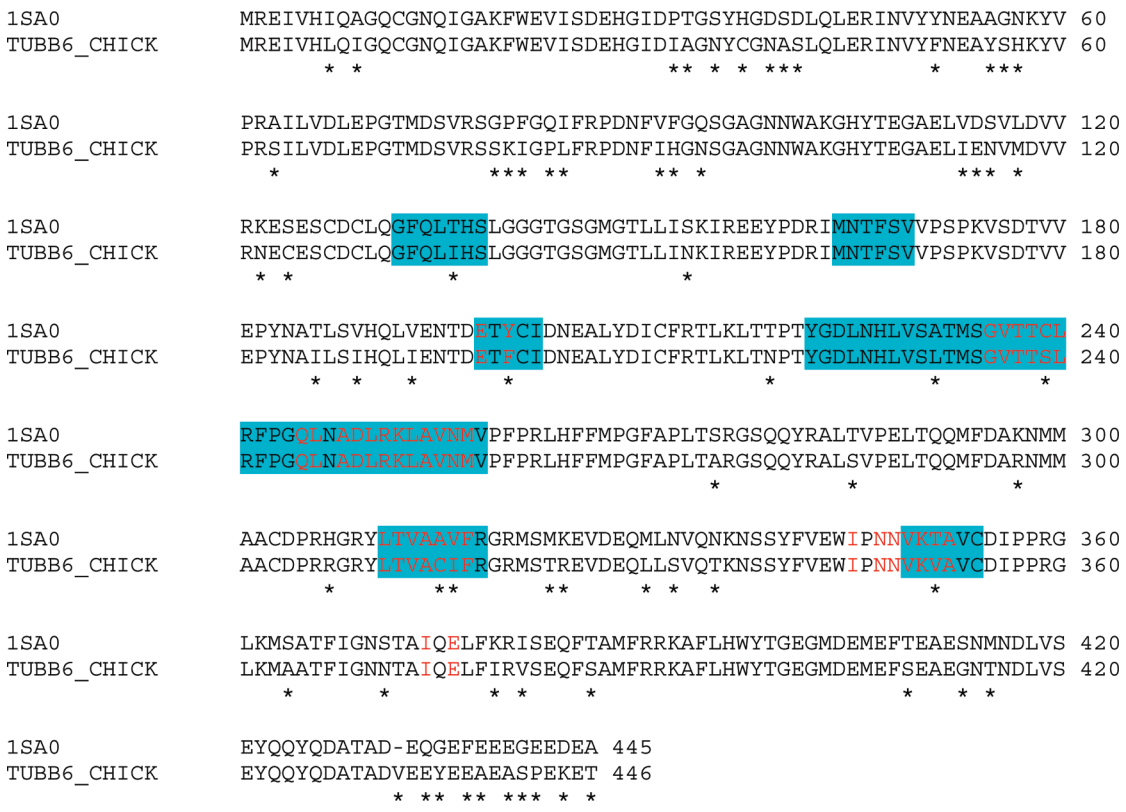

FIGURE 2: Sequence alignment of the β-subunit of 1SA0 and *Gallus gallus* isotype βVI. Residues colored red are those that were within 6 Å of the binding site. Residues highlighted in cyan are those in the colchicine binding domain. Mutations are marked with an asterisk underneath the alignment.

allocolchicine to CeTb in the presence and absence of podophyllotoxin. A solution of CeTb (1 μM) in PME containing 0.1 mM GTP was incubated with 150 μM podophyllotoxin in the fluorescence cell at 25 °C for 25 min. Allocolchicine was added to a final concentration of 150 μM, and the kinetics of binding were followed as described above. The DMSO concentration was limited to 10%. For a reasonable comparison, a similar experiment was performed with BbTb except that the concentrations of podophyllotoxin and allocolchicine were 50 μM each.

Sequence Alignment and Structural Superimposition of Chicken Erythrocyte Tubulin on Mammalian Brain Tubulin (*Protein Data Bank entry 1SA0*). The sequence and structure of BbTb bound to colchicine was downloaded from the RSCB Protein Data Bank (entry 1SA0). The sequences of chicken tubulin isotype βVI and human isotype β1 were downloaded from the NCBI database (accession numbers P09207 and NP_110400, respectively). Linear sequence alignment was performed using Clustal W2 (European Bioinformatics Institute). The 1SA0 coordinates of the $\alpha\beta$ dimer including GTP, GDP, and colchicine (SH group of the CN2 ligand replaced by H) were used as starting coordinates for minimization of the mammalian brain tubulin dimer. For the minimization of the avian βVI dimer (α1, βVI), substitutions were made in the 1SA0 β-chain using the sequence of the chicken isotype βVI and the α-chain was kept the same as in the 1SA0 structure. The AMBER 9 suite of programs (Scripps Research Institute) was used to perform the minimizations. To neutralize the systems, 33 and 31 Na^+ ions were added to the mammalian brain and avian βVI dimer structures, respectively. Both structures were immersed in TIP3P boxes of water extending 15 Å from the surface of the dimers. The minimizations were performed using periodic boundary conditions. The minimized chicken erythrocyte tubulin structure was superimposed on the minimized mammalian brain tubulin structure using the DS Visualizer from Accelrys (San Diego, CA). Residues belonging to the β-chains within 6 Å of any atoms of the colchicine were identified in both proteins. Both three-dimensional structures were aligned, and the extended colchicine binding domains, encompassing the S4−S6, S8, and S9 sheets, the H7 and H8 helices, and the T7 loop as described by Ravelli et al. (*40*), were searched for divergent residues.

We considered only the β-subunits of the proteins for our study because the α-subunits do not differ significantly across the isotypes (*4*). Additionally, we aligned isotype α1 of chicken tubulin with the α-subunit of 1SA0 and did not observe any difference in α-tubulin sequence close to the colchicine binding site.

RESULTS

Linear Alignment and Structure Superimposition. Linear sequence alignment of the avian tubulin βVI chain with the β-chain of 1SA0 reveals 67 divergent residues across the entire length of avian βVI (Figure 2), the highest proportion of which is in the hypervariable C-terminus. A three-dimensional structure for avian βVI-tubulin was constructed from the 1SA0 crystal structure as described in Materials and Methods. Three-dimensional structure superimposition of the two β-tubulin chains shows that a total of 36 residues fall within 6 Å of colchicine. This region is comprised of residues 198, 200, 235−240, 245, 246, 248−257, 311−317, 345, 347−352, 374, and 376. Of these 36 residues, five substitutions are observed in isotype βVI: Y200F, C239S, A315C, V316I, and T351V (Figure 3). The divergent residues are located in helices H7 and H8 and sheets S8 and S9 (Figures 2 and 3). The alignment shows two further mutations in the extended colchicine binding domain: T136I in S4 and A231L in H7 (Figure 2).

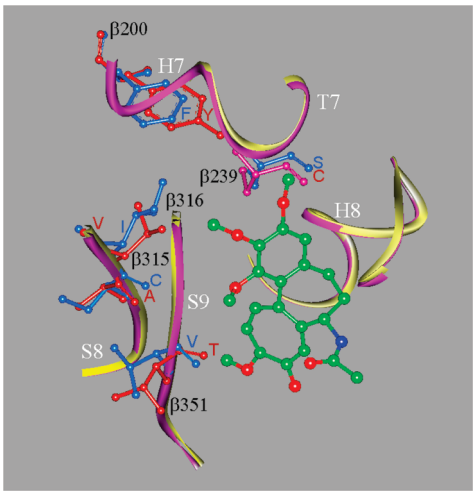

FIGURE 3: Schematic diagram of differences in mammalian brain β-tubulin (from the 1SA0 structure) and isotype βVI of chicken in the colchicine binding site. The 1SA0-derived coordinates of the α/β-heterodimer including GTP, GDP, and colchicine (SH group replaced by H) were used as starting coordinates for the minimization procedure for the mammalian brain tubulin dimer. The chicken erythrocyte tubulin dimer was created from 1SA0, and the two dimers were minimized and superimposed as described in Materials and Methods. The residues containing any atom within 6 Å of bound colchicine were selected. Only the divergent residues within this cutoff are shown in small ball-and-stick representations colored blue (chicken isotype βVI) and brown (mammalian brain β-tubulin). The helices, β-sheets, and loops for mammalian brain β-tubulin and chicken isotype βVI are shown as purple and yellow ribbons, respectively. The colchicine is shown in a large ball-and-stick representation with C, O, and N atoms colored green, red, and dark blue, respectively. Only the mammalian structure colchicine is shown as it differs only slightly from the colchicine in the chicken βVI structure. Five substitutions (Y200F, C239S, A315C, V316I, and T351V) were observed in chicken isotype βVI relative to mammalian brain β-tubulin within the 6 Å cutoff.

The colchicine binding region defined here differs slightly from that assigned by Huzil et al., which contains 29 amino acids (*41*). The only significant difference between the two models is that the Y200F substitution is not included in their binding site sequence.

Effect of Colchicine on CeTb Polymerization. The effect of colchicine on the ability of CeTb to assemble in the presence of paclitaxel was investigated and compared to that of BbTb under identical conditions. CeTb has a lower critical concentration than BbTb and has a stronger tendency to form oligomers, which slow the rate of assembly (*26*, *27*). To minimize the amount of oligomers in solution, low tubulin concentrations were employed. CeTb assembled in the presence of paclitaxel formed normal microtubules, which was confirmed by electron microscopy (data not shown). CeTb and BbTb assembly was monitored by apparent light scattering as described in Materials and Methods. Colchicine decreased both the rate and extent of BbTb assembly, as expected (data not shown). Colchicine did not, however, affect either the rate or extent of CeTb polymerization at any of the concentrations tested. No inhibition of CeTb polymerization was observed at colchicine concentrations up to 140 μM (Figure 4A). A well-defined dose−response curve (Figure 4B) yields an IC_{50} of 2.7 ± 0.03 μM for BbTb (Table 1).

Kinetics of Binding of Colchicine to CeTb. Two possibilities were considered for the absence of an inhibitory effect of colchicine on CeTb assembly: either the ligand does not bind well to the colchicine site, or binding occurs but the resulting complex

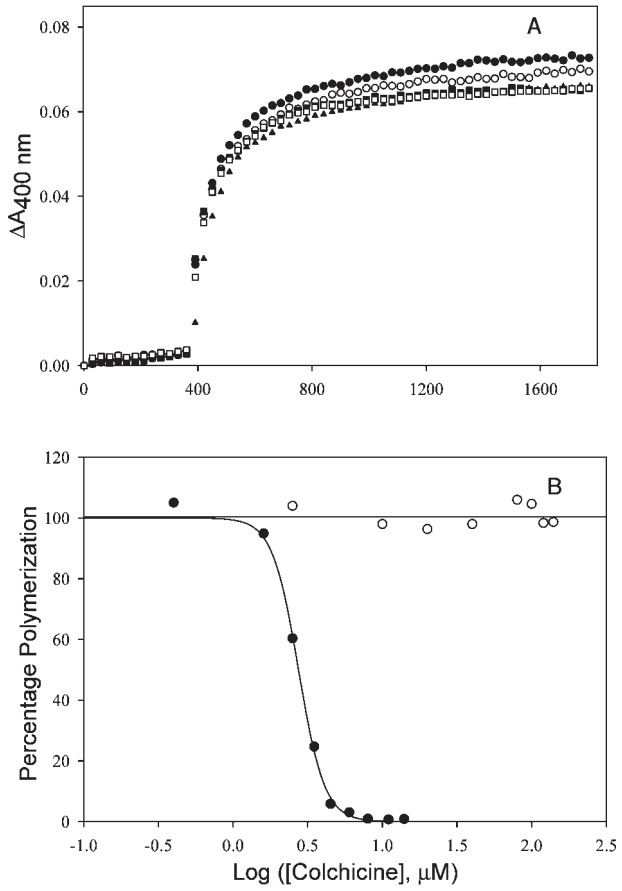

FIGURE 4: (A) Effect of colchicine on paclitaxel-induced polymerization of CeTb. CeTb (5 μM) in PME and 0.1 mM GTP was incubated with increasing concentrations of colchicine for 90 min at 25 °C. The samples were then treated with paclitaxel (5 μM) at 37 °C, and the polymerization was monitored in terms of the apparent absorption at 400 nm. The colchicine concentrations were 0 (▲), 80 (●), 100 (○), 120 (■), and 140 μM (□). (B) Plot for IC_{50} values of colchicine for BbTb (●) and Cetb (○). The IC_{50} of BbTb was 2.7 μM, and that for CeTb was > 140 μM.

Table 1: Inhibition of Paclitaxel-Induced Assembly of BbTb or CeTb by Colchicine Site Ligands

		IC_{50} (μM)	
ligand	[tubulin] (μM)	BbTb	CeTb
colchicine	5	2.7 ± 0.03	≫140
podophyllotoxin	5	1.6 ± 0.02	25 ± 1
nocodazole	5	7.7 ± 0.2	87 ± 2
allocolchicine	5	2.2 ± 0.09	ND[a]
allocolchicine	2	0.5	5

[a]No inhibition of assembly observed at the solubility limit under these experimental conditions (40 μM).

does not inhibit CeTb assembly. Colchicine fluorescence emission intensity is enhanced, and tubulin fluorescence is quenched upon formation of the complex (*12*). Therefore, both signals were probed to detect colchicine binding to CeTb. The results were compared to those from colchicine binding to BbTb under identical conditions. Figure 5A shows that there is negligible enhancement in the fluorescence of colchicine upon incubation with CeTb relative to that with BbTb. Tubulin-bound fluorescence of colchicine is due in part to a highly rigid environment for the ligand after binding (*42*), which may be the difference for

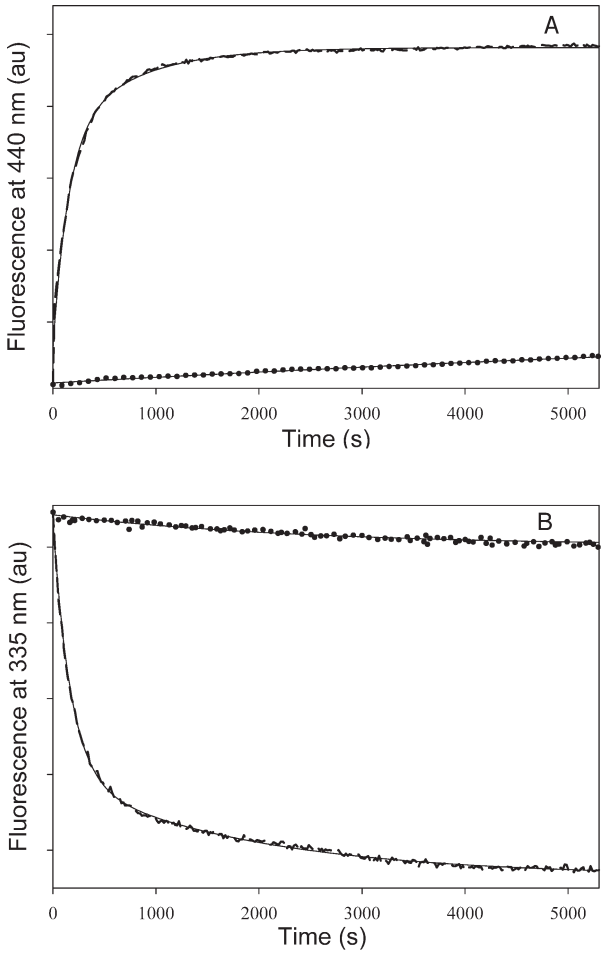

FIGURE 5: (A) Effect of BbTb (---) and CeTb (···) on the fluorescence of colchicine. Tubulin (1 μM) was added to colchicine (150 μM) in PME in the presence of 0.1 mM GTP at 25 °C, and the enhancement of colchicine fluorescence at 440 nm was monitored as a function of time. (B) Effect of colchicine on the intrinsic fluorescence of BbTb (---) and CeTb (···). Colchicine (150 μM) was added to tubulin (1 μM) in PME in the presence of 0.1 mM GTP at 25 °C, and the quenching of the intrinsic protein fluorescence at 335 nm was monitored as a function of time.

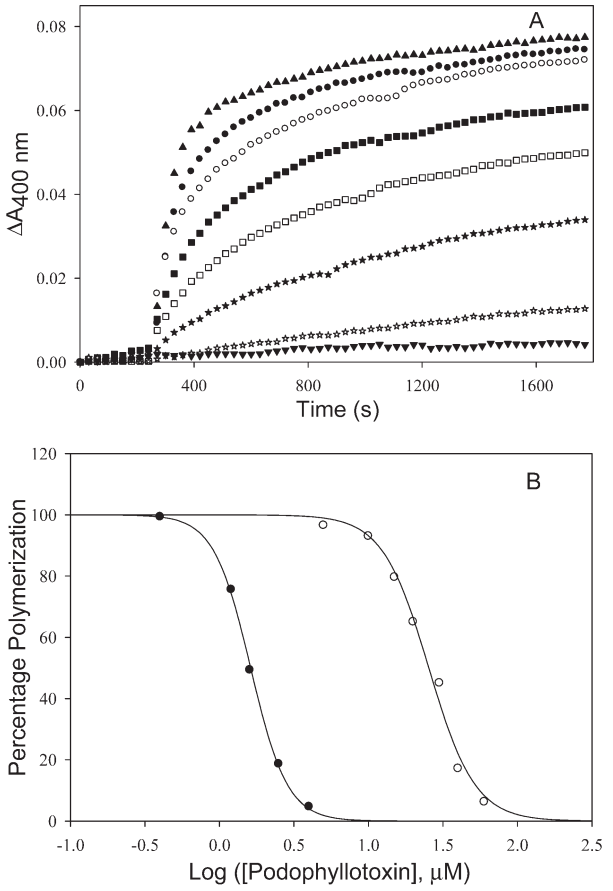

FIGURE 6: (A) Effect of podophyllotoxin on paclitaxel-induced polymerization of CeTb. CeTb (5 μM) in PME and 0.1 mM GTP was incubated with increasing concentrations of podophyllotoxin for 25 min at 25 °C. The samples were then treated with paclitaxel (5 μM) at 37 °C, and the polymerization was monitored in terms of the apparent absorption at 400 nm. The podophyllotoxin concentrations were 0 (▲), 5 (●), 10 (○), 15 (■), 20 (□), 30 (★), 40 (☆), and 60 μM (▼). (B) Plot of the IC_{50} values of podophyllotoxin for BbTb (●) and Cetb (○). The IC_{50} of BbTb was 1.6 μM, and that for CeTb was 25 μM.

CeTb. Many colchicine site ligands quench BbTb fluorescence, and this signal may also be used to monitor ligand binding (*12*). Colchicine does not, however, significantly quench the intrinsic fluorescence of CeTb (Figure 5B). Both of these results indicate a lack of colchicine binding to CeTb.

Effect of Podophyllotoxin on Paclitaxel-Induced Tubulin Assembly. Unassembled CeTb may contain a substantial amount of oligomers, particularly at high protein concentrations (*25*). Colchicine binds to soluble tubulin but not to microtubules (*43*). Therefore, one explanation for the lack of colchicine binding activity in CeTb is that the aggregation state of the protein in CeTb does not allow access to the colchicine binding site. Schönbrunn et al. showed that podophyllotoxin is able to dissolve CeTb ring aggregates, and they concluded that podophyllotoxin is probably able to bind to tubulin aggregates (*44*). The effect of podophyllotoxin on the assembly of CeTb was therefore assessed. Figure 6A shows that podophyllotoxin causes a concentration-dependent decrease in the degree of CeTb assembly, and the data fit a normal dose−response curve (Figure 6B). The IC_{50} for podophyllotoxin inhibition of CeTb assembly is ~15-fold greater than that determined for BbTb under the same experimental conditions (Table 1).

Effect of Nocodazole on Paclitaxel-Induced Tubulin Assembly. Nocodazole is an antimicrotubule agent without apparent structural similarity to colchicine that is a competitive inhibitor of binding of colchicine to tubulin (*45*). Like that of colchicine, the affinity of nocodazole for tubulin varies with the β-tubulin isotype, and each drug binds with the lowest affinity to $\alpha\beta$III-tubulin (*18*, *21*). It was therefore of interest to determine whether the similarity between nocodazole and colchicine binding would extend to the predominant αI/βVI isotype in CeTb. The effect of nocodazole on CeTb and BbTb assembly was assessed (Figure 7). Nocodazole is less potent than podophyllotoxin as an inhibitor of CeTb assembly (Table 1), but the difference in the effect of the drug on CeTb and BbTb assembly is smaller for nocodazole (~11-fold) than for podophyllotoxin (~15-fold).

Effect of Allocolchicine on CeTb Polymerization. Allocolchicine is a structural isomer of colchicine whose interaction with BbTb has been thoroughly documented (*36*, *46*). Overall, the characteristics of the associations of the two molecules with BbTb are very similar, but the mechanistic steps to form the final complexes are significantly different. The effect of allocolchicine on the assembly of CeTb was therefore examined. The IC_{50} of CeTb assembly inhibition by allocolchicine could not be quantified

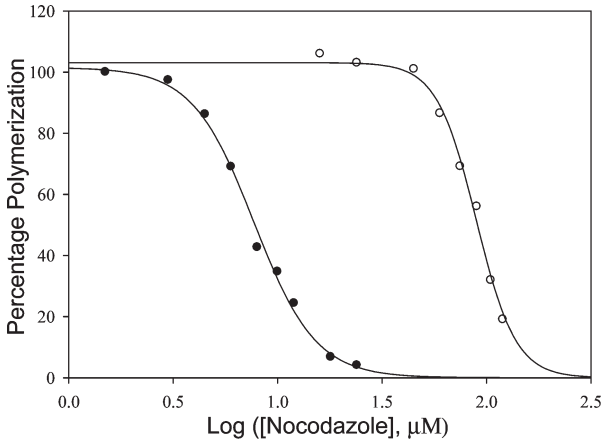

FIGURE 7: Plot of IC_{50} values of nocodazole for BbTb (●) and Cetb (○). Tubulin (5 μM) in PME and 0.1 mM GTP was incubated with increasing concentrations of nocodazole for 40 min at 25 °C. The samples were then treated with paclitaxel (5 μM) at 37 °C, and the polymerization was monitored in terms of the apparent absorption at 350 nm. The IC_{50} of nocodazole for BbTb was 7.7 μM, and that for CeTb was 87 μM.

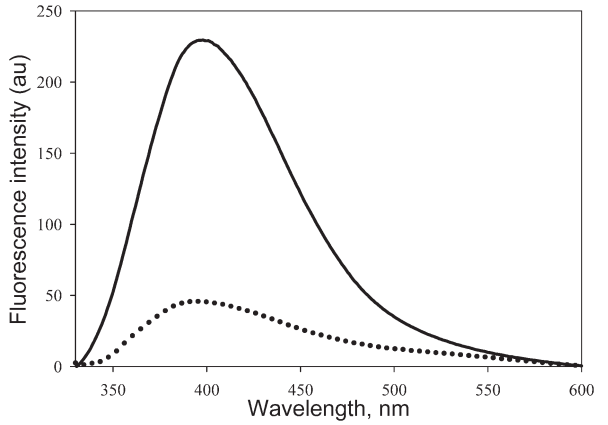

FIGURE 8: Emission spectra of allocolchicine in the presence of BbTb (—) and CeTb (···). Allocolchicine (150 μM) was incubated with tubulin (1 μM) at 25 °C for 90 min, and the ligand emission spectra were recorded via excitation of the samples at 315 nm.

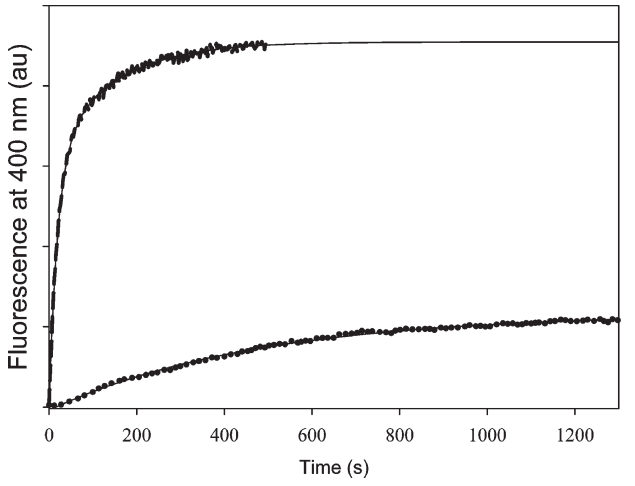

FIGURE 9: Enhancement of allocolchicine fluorescence upon binding of BbTb (---) and CeTb (···) as a function of time. Tubulin (1 μM) was added to an allocolchicine solution (150 μM) at 25 °C. The excitation and emission wavelengths were 330 and 400 nm, respectively. The kinetics of binding were evaluated as described in Materials and Methods.

because of the limited solubility of the ligand under the experimental conditions (5 μM CeTb and 2% DMSO). However, when the tubulin concentration was decreased to 2 μM, inhibition of tubulin assembly by allocolchicine was observed at soluble concentrations (Figure S1 of the Supporting Information). We found that 20 μM allocolchicine causes complete inhibition of 2 μM CeTb assembly in the presence of 2 μM paclitaxel. The IC_{50} value for allocolchicine inhibition of 2 μM CeTb assembly is ~10-fold greater than the IC_{50} for BbTb under the same conditions (Table 1).

Association of Allocolchicine with CeTb. The association of allocolchicine with CeTb was studied in terms of the effect of CeTb on allocolchicine fluorescence, and the data were compared with those of allocolchicine binding to BbTb. Like colchicine, the fluorescence of allocolchicine is dramatically enhanced upon binding to bovine brain tubulin. Unlike colchicine, the fluorescence properties of the tubulin-bound species can be emulated by solvent (*36*). The effect of CeTb and BbTb on the fluorescence of allocolchicine was compared (Figure 8). Both sources of tubulin enhance the fluorescence of allocolchicine. The emission intensity of allocolchicine in the presence of CeTb is ~5-fold lower than that of allocolchicine with BbTb under identical experimental conditions. The lower intensity of allocolchicine with CeTb could be due to a number of factors: a difference in the association constants of allocolchicine for the two tubulins, differences in the quantum yields of the complexes, the presence of inactive forms of CeTb in the solution, or a combination of these. Note that the emission maximum of allocolchicine with CeTb is blue-shifted 5 nm from that of allocolchicine with BbTb, which indicates that the environment experienced by allocolchicine with CeTb is more hydrophobic than its environment in the colchicine binding site of BbTb (*36*). This observation is in agreement with the amino acid substitutions in the isotype βVI binding site, which is considerably more hydrophobic than that of isotypes βI, βII, and βIV (grand averages of hydrophobicity for YCAVT and FSCIV of 1.30 and 2.64, respectively).

The difference in the fluorescence intensity of bound allocolchicine over that of the free ligand allows the ligand emission at 400 nm to be used to monitor its association with tubulin. The association kinetics of allocolchicine with CeTb and BbTb were studied under pseudo-first-order conditions by monitoring the increase in ligand emission intensity as a function of time. As seen in Figure 9, allocolchicine binding to BbTb is much faster than allocolchicine binding to CeTb. Under identical conditions, the binding with BbTb attains a plateau within 600 s, whereas that with CeTb attains a plateau within 1300 s. The association of allocolchicine with CeTb is also monophasic, whereas the association with BbTb is biphasic, as expected. At 25 °C, the association rate constant for CeTb is 14.5 ± 0.09 M^{-1} s^{-1} (Table 2). For BbTb, the association rate constant for the fast phase of allocolchicine binding is 343 ± 7 M^{-1} s^{-1} (Table 2), which is in accordance with previous experimental results (*36*).

Enhancement of allocolchicine fluorescence upon tubulin binding was also used to assess the affinity of allocolchicine for CeTb. Emission intensity was recorded as a function of allocolchicine concentration with a fixed concentration of tubulin at 25 °C. The fluorescence enhancement plateaus at 150 μM for 1 μM CeTb (Figure 10). A similar experiment with BbTb shows that that fluorescence enhancement of plateaus at ~20 μM (Figure 10). The fluorescence titrations of allocolchicine binding to CeTb and BbTb were fit to a single-site isotherm, which yielded association constants of 0.18×10^5 and 5.0×10^5 M^{-1} for CeTb and BbTb, respectively.

Table 2: Association Rate Constants of the Binding of Colchicine, Allocolchicine, Thiocolchicine, and Chlorocolchicine to BbTb and CeTb

drug	k_f (M^{-1} s^{-1})[a] for BbTb	k (M^{-1} s^{-1})[b] for CeTb
colchicine	45.3 ± 0.7	–
allocolchicine	343 ± 7	14.5 ± 0.09
thiocolchicine	129 ± 5	2.20 ± 0.03
chlorocolchicine	367 ± 7	11.7 ± 0.4

[a] k_f is the apparent second-order rate constant of the fast phase of biphasic binding. All measurements were performed at 25 °C as described in Materials and Methods. [b] k is the second-order rate constant for monophasic binding. All measurements were performed at 25 °C as described in Materials and Methods.

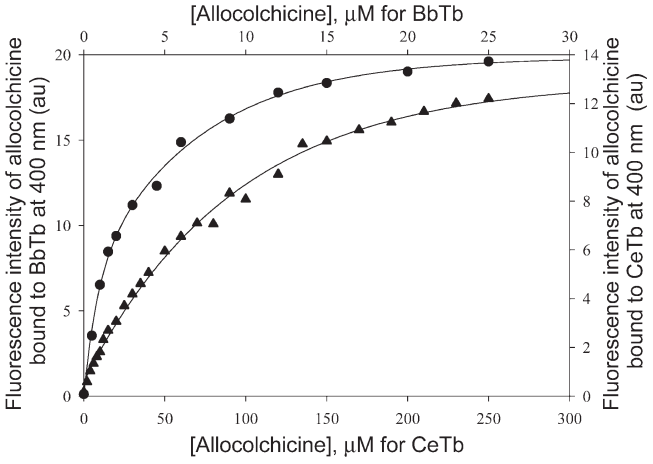

FIGURE 10: Enhancement of allocolchicine fluorescence upon binding to BbTb (●) and CeTb (▲) at 25 °C as a function of ligand concentration. The excitation wavelength was 315 nm. Spectra were recorded as described in Materials and Methods.

Inhibition of Allocolchicine Binding to CeTb by Podophyllotoxin. Comparing the characteristics of allocolchicine binding to CeTb to those of allocolchicine binding to BbTb assumes that the ligand is occupying the colchicine binding site on both proteins. Since podophyllotoxin is a competitive inhibitor of colchicine binding to BbTb (*47*), the effect of podophyllotoxin on allocolchicine binding to CeTb was assessed. Figure 11 shows the kinetics of association of allocolchicine with CeTb or BbTb in the presence and absence of podophyllotoxin. Preincubation of tubulin with podophyllotoxin causes complete inhibition of allocolchicine binding to CeTb.

Kinetics of Binding of Chlorocolchicine and Thiocolchicine to BbTb and CeTb. The difference between the CeTb-inactive molecule colchicine and the CeTb-active molecule allocolchicine is the structure of the C ring. We explored whether a less dramatic alteration in the C ring region of a colchicinoid could produce a molecule with CeTb activity. Thiocolchicine (Figure 1) differs from colchicine by one atom in the C ring substitutent; this alteration slightly increases the rate constant and equilibrium constant for BbTb binding (*30*). Chlorocolchicine (10-demethoxy-10-chlorocolchicine) is slightly more potent than colchicine as an inhibitor of BbTb assembly (*29*). The rates of the three colchicinoids binding to tubulin at a single concentration and temperature were measured under pseudo-first-order conditions (20 μM colchicinoid and 1 μM BbTb). Figure 12A shows the kinetic traces of the ligands binding to BbTb. The biphasic curves for ligands binding to BbTb were fit to the appropriate equation (see

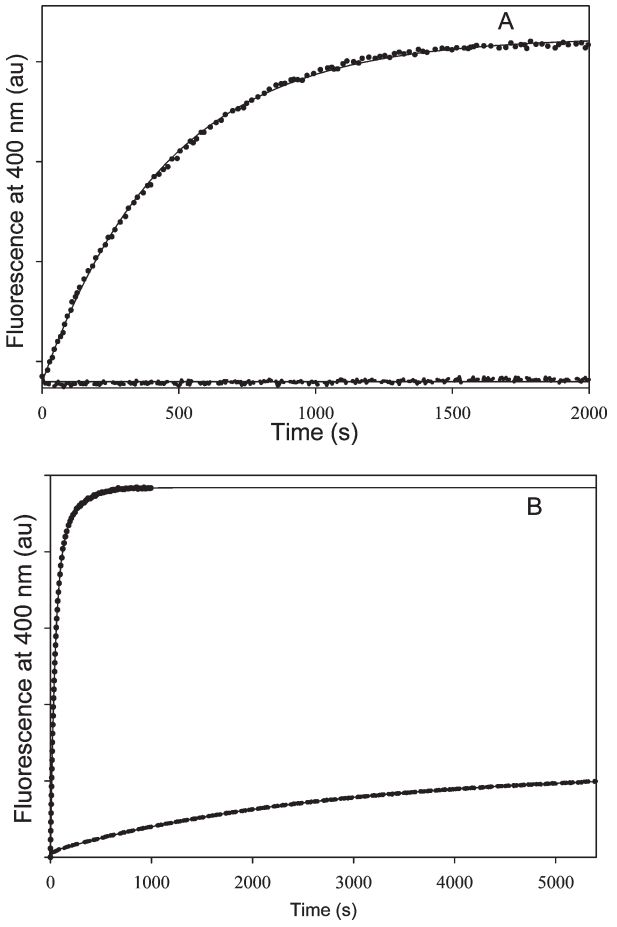

FIGURE 11: Competition of allocolchicine binding to tubulin by podophyllotoxin. The kinetics of allocolchicine binding to CeTb (A) and BbTb (B) in the absence (···) and presence (---) of podophyllotoxin were measured. CeTb (1 μM) was incubated with 0 and 150 μM podophyllotoxin for 25 min at 25 °C. At the end of the incubation, allocolchicine (150 μM) was added to the solution and binding was studied in terms of the increase in allocolchicine fluorescence as a function of time. For the experiment with BbTb, each ligand at 50 μM was used. DMSO was limited to 10%. The excitation and emission wavelengths were 330 and 400 nm, respectively.

Materials and Methods), and the second-order rate constants of the fast phase were calculated (Table 2). The kinetic experiments were repeated with CeTb (Figure 12B), except that the ligand concentration was increased to 150 μM. Colchicine caused very little quenching of CeTb fluorescence over the nearly 2 h period of the experiment; however, the data for the two other colchicinoids could be fit to a single-exponential decay, and rate constants were calculated (Table 2). Under these experimental conditions, the binding rates for the colchicinoids are in the following order for both sources of tubulin: chlorocolchicine > thiocolchicine > colchicine.

DISCUSSION

Colchicine binding to mammalian tubulin is both unique and ubiquitous. The specificity of colchicine binding to tubulin over all other cellular proteins was demonstrated when tubulin was first identified as the primary protein of the microtubule as well as the colchicine binding protein in the cell. All mammalian tubulin examined to date is able to bind colchicine (*12*). The idea that there might be some heterogeneity in mammalian tubulins toward colchicine was confirmed by Ludueña's group, who

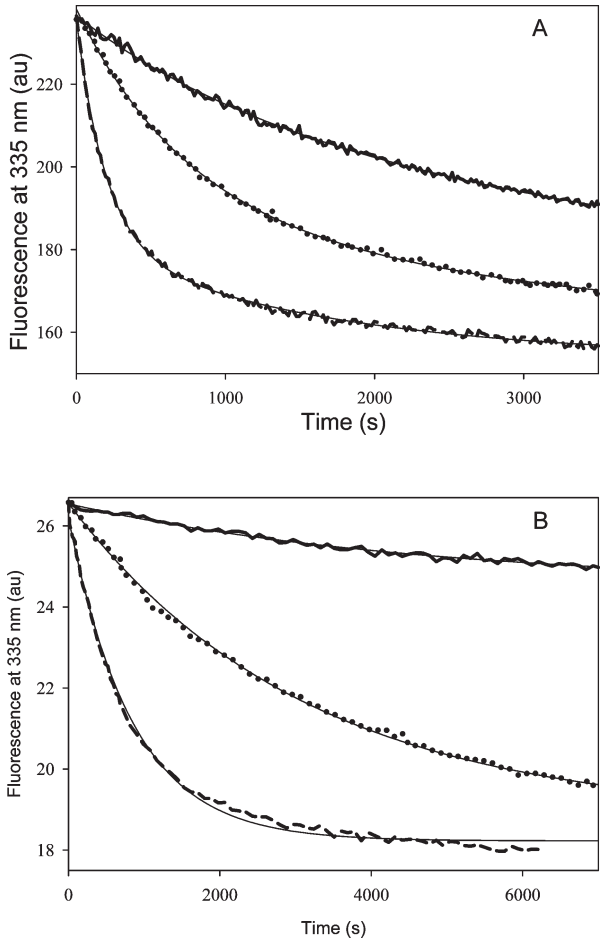

FIGURE 12: Quenching of the intrinsic fluorescence of BbTb (A) and CeTb (B) by colchicine (—), thiocolchicine (· · ·), and chlorocolchicine (---), as a function of time. Ligands were added to tubulin solutions to yield final concentrations of 1 μM tubulin and 20 μM ligands in panel A and 1 μM tubulin and 150 μM ligands in panel B at 25 °C. The excitation and emission wavelengths were 295 and 335 nm, respectively.

developed antibodies to different β-tubulin isotypes. The second kinetic phase for colchicine binding to brain tubulin was shown to be due to isotype βIII, which makes up ~25% of neural β-tubulin (*48*). Equilibrium binding data show that molecules that bind to the colchicine site on tubulin also bind with different affinities to various β-isotypes (*18*, *21*, *49*). A common theme of the colchicine site binding ligands is that the slowest, weakest binding occurs with isotype βIII. This is the most diverse isotype in tubulins isolated from mammalian brain and is the only one that shows heterogeneity at the colchicine binding site. The colchicine binding site of isotype βIII, defined as a region within 6 Å of colchicine, differs from isotypes βI, βII, and βIV at three positions: C239S, A315T, and T351V. Biochemical studies have identified C239 as an important amino acid in the binding site (*50*), and Joe et al. propose that this difference could be a key feature in the lower affinity of isotype βIII for colchicine (*51*). Huzil et al. postulate that replacement of the smaller amino acids A315 and T351 with T and V, respectively, may cause disruption in the interactions with adjacent helices 9 and 10, resulting in an overall narrowing of the colchicine binding site and thereby reducing the affinity for colchicine (*41*).

Our modeling of isotype βVI identifies five substitutions in the colchicine binding site (Y200F, C239S, A315C, V316I, and T351V) that are located in helices H7 and H8, sheets S8 and S9, and loop T7. The three variant positions in isotype βIII are also different in isotype βVI, although the amino acid at position 315 is C in isotype βVI and T in isotype βIII. Within the colchicine binding site, the differences between isotype βIII and isotype βVI are very subtle: loss of a hydroxyl (Y to F), addition of a methyl (V to I), and substitution of an oxygen with a sulfur atom (T to C). Yet these changes are sufficient to render colchicine binding to isotype βVI undetectable. The apparent lack of colchicine binding to CeTb therefore may be due in part to a further narrowing of the colchicine binding site relative to that of isotype βIII by the additional methyl group at position 316 and the larger sulfur atom at position 315.

The A ring of colchicine has been described as an "anchor" for the placement of the C ring of the molecule within the binding site (*52*). The effect of a colchicine site ligand on the tubulin conformation is dictated by interactions between the C ring domain of the binding site on tubulin and the inhibitor. Podophyllotoxin and colchicine exemplify this statement. Both ligands produce the same end result, inhibition of tubulin assembly, by binding to the same region of the protein. However, the path by which the inhibitory complex is formed and the nature of the final complex are very different for the two ligands. Colchicine binds to tubulin in a two-step process that is revealed by evaluation of the concentration dependence of the apparent second-order rate constant (*15*). A tubulin conformational change occurs in the slow unimolecular second step of the process, and this conformational change can be detected by multiple techniques. In contrast, podophyllotoxin binds to tubulin in a single bimolecular reaction (*47*), and the conformation of the podophyllotoxin−tubulin complex cannot be differentiated from that of unliganded tubulin by direct means (e.g., spectroscopic changes or tubulin GTPase activity) (*14*).

Although they share a common structural feature, podophyllotoxin and colchicine do not occupy the binding site on tubulin in the same way. In fact, the trimethoxyphenyl rings of colchicine and podophyllotoxin bound to tubulin are almost perpendicular to each other in the crystal structures (see Figure S2 of the Supporting Information). Colchicine derivatives, though, would be expected to have very similar orientations in the binding site because of the high rigidity of the fused tricyclic scaffold. The constricted nature of the A ring domain of the CeTb binding site may not allow the molecule to penetrate as deeply into the protein, and thus, stabilizing interactions between the tropone ring and the protein may not be accessible to the ligand in the narrower βVI-tubulin binding site. Allocolchicine may be able to make some productive contacts with the protein because of the relatively flexible methyl ester and therefore possess some CeTb binding activity. The C-10 substituent of thiocolchicine is larger than the methoxy group of colchicine, but the C-10 heteroatoms of both thio- and chlorocolchicine are more polarizable, which may account for the weak CeTb binding observed for these two ligands.

The data presented here may have a bearing on clinical applications of colchicine site drugs. It has previously been suggested that hematopoetic mammalian β1-tubulin[2] is the equivalent of avian βVI, but it was also observed that the two proteins contained many differences in amino acid sequence (*53*). When the sequences for human β1 (NP_110400) and avian βVI (P09207) are aligned, we find that, although there is significant

[2]Not the same as class Iβ, which is also called βI in some nomenclature systems. See ref *5* for a discussion of tubulin isotype nomenclature.

sequence divergence, the colchicine binding site and the colchicine binding domain as defined in this work contain only one nonconservative mutation (Figure S3 of the Supporting Information). In mammals, β1-tubulin expression occurs in mature megakaryocytes and blood platelets, up to 90% of the total β-tubulin content in these cells being isoform β1 (*54*). Transgenic mice lacking β1-tubulin have fewer platelets than wild-type mice (*24*). These platelets also have reduced microtubule content and are structurally and functionally defective. It has long been known that one of the side effects of many microtubule-active drugs is myelosuppression, and it is possible that the hematological toxicity of these drugs may be the result of their effect on microtubules of hematopoietic cells (*55*, *56*). Although there are differences in the overall sequences of the two β-tubulins (16% nonidentical), only two of the 36 amino acids surrounding the colchicine binding site on βVI-tubulin are different in human β1-tubulin: Val236 and Glu198 in chicken βVI-tubulin are Ile and Ala in human β1-tubulin, respectively. It stands to reason that human β1 may exhibit the same divergent ligand binding behavior seen in avian βVI. Indeed, it has recently been shown that cells containing human β1 are insensitive to the colchicine binding site ligand 2-methoxyestradiol (*57*). Thus, measurements of ligand binding to CeTb may provide a way to predict the hematological toxicity of potential new colchicine site drugs and a screen for potential molecules for targeted chemotherapy of hematopoietic cell disorders.

CONCLUSION

In this paper, we have provided evidence that avian βVI-tubulin possesses unique drug binding characteristics with respect to the colchicine site that are remarkably different from those of any other higher-order eukaryotic tubulin studied to date. We could not find any evidence of colchicine binding up to the concentrations tested in any of our assays. Whether CeTb will bind colchicine at higher concentrations is currently under investigation in our lab, but regardless, it is at least the first report of a higher eukaryotic tubulin that exhibits this behavior.

Interestingly, although the colchicine site in avian βVI does not appear to bind colchicine, it maintains an ability to bind to other colchicine site ligands, which also inhibit microtubule polymerization. This suggests that the binding site on βVI has not lost function but is simply different from the site on other tubulins with regard to shape, electronics, or both. With this in mind, it is possible that small molecules can be found which will preferentially bind to the avian βVI tubulin over other tubulins. This could translate into a targeting mechanism for hematopoietic tissue in vivo.

NOTE ADDED AFTER ASAP PUBLICATION

After this paper was published ASAP March 3, 2010, corrections were made to Figures 9 and 10. The revised version was reposted March 10, 2010.

SUPPORTING INFORMATION AVAILABLE

Inhibition of paclitaxel-induced CeTb assembly by allocolchicine, an illustration of the three-dimensional alignment of tubulin-bound colchicine and podophyllotoxin, and sequence alignment of chicken erythrocyte βVI-tubulin and human β1-tubulin. This material is available free of charge via the Internet at http://pubs.acs.org.

REFERENCES

1. Morejohn, L. C., and Fosket, D. E. (1991) The biochemistry of compounds with anti-microtubule activity in plant cells. *Pharmacol. Ther. 51*, 217–230.
2. Kohler, P. (2001) The biochemical basis of anthelmintic action and resistance. *Int. J. Parasitol. 31*, 336–345.
3. Jordan, A., Hadfield, J. A., Lawrence, N. J., and McGown, A. T. (1998) Tubulin as a target for anticancer drugs: Agents which interact with the mitotic spindle. *Med. Res. Rev. 18*, 259–296.
4. Luduena, R. F. (1998) Multiple forms of tubulin: Different gene products and covalent modifications. *Int. Rev. Cytol. 178*, 207–275.
5. Verdier-Pinard, P., Pasquier, E., Xiao, H., Burd, B., Villard, C., Lafitte, D., Miller, L. M., Angeletti, R. H., Horwitz, S. B., and Braguer, D. (2009) Tubulin proteomics: Towards breaking the code. *Anal. Biochem. 384*, 197–206.
6. Jordan, M. A., and Wilson, L. (1998) Microtubules and actin filaments: Dynamic targets for cancer chemotherapy. *Curr. Opin. Cell Biol. 10*, 123–130.
7. Dumontet, C., Jordan, M. A., and Lee, F. F. Y. (2009) Ixabepilone: Targeting βIII-tubulin expression in taxane-resistant malignancies. *Mol. Cancer Ther. 8*, 17–25.
8. Katsetos, C. D., Herman, M. M., and Mork, S. J. (2003) Class III β-tubulin in human development and cancer. *Cell Motil. Cytoskeleton 55*, 77–96.
9. Ferrandina, G., Zannoni, G. F., Martinelli, E., Paglia, A., Gallotta, V., Mozzetti, S., Scambia, G., and Ferlini, C. (2006) Class III β-tubulin overexpression is a marker of poor clinical outcome in advanced ovarian cancer patients. *Clin. Cancer Res. 12*, 2774–2779.
10. Seve, P., Reiman, T., Lai, R., Hanson, J., Santos, C., Johnson, L., Dabbagh, L., Sawyer, M., Dumontet, C., and Mackey, J. R. (2007) Class III β-tubulin is a marker of paclitaxel resistance in carcinomas of unknown primary site. *Cancer Chemother. Pharmacol. 60*, 27–34.
11. Pepe, A., Sun, L., Zanardi, I., Wu, X. Y., Ferlini, C., Fontana, G., Bombardelli, E., and Ojima, I. (2009) Novel C-seco-taxoids possessing high potency against paclitaxel-resistant cancer cell lines overexpressing class III β-tubulin. *Bioorg. Med. Chem. Lett. 19*, 3300–3304.
12. Hastie, S. B. (1991) Interactions of colchicine with tubulin. *Pharmacol. Ther. 51*, 377–401.
13. Haber, J. E., Peloquin, J. G., Halvoroson, H. O., and Borisy, G. G. (1972) Colcemid inhibition of cell growth and the characterization of a colcemid-binding activity in *Saccharomyces cerevisiae*. *J. Cell Biol. 55*, 355–367.
14. Bane, S. (2007) Molecular features of the interaction of colchicine and related structures with tubulin. In Microtubule Targets in Cancer Therapy: The Role of Microtubules in Cell Biology, Neurobiology, and Oncology (Fojo, A., Ed.) pp 260−280, Humana Press, Totowa, NJ.
15. Garland, D. L. (1978) Kinetics and mechanism of colchicine binding to tubulin: Evidence for ligand-induced conformational change. *Biochemistry 17*, 4266–4272.
16. Banerjee, A., and Luduena, R. F. (1991) Distinct colchicine binding-kinetics of bovine brain tubulin lacking the type-III isotype of β-tubulin. *J. Biol. Chem. 266*, 1689–1691.
17. Banerjee, A., Dhoore, A., and Engelborghs, Y. (1994) Interaction of desacetamidocolchicine, a fast binding analog of colchicine with isotypically pure tubulin dimers α-β(II), α-β(III) and α-β(IV). *J. Biol. Chem. 269*, 10324–10329.
18. Banerjee, A., and Luduena, R. F. (1992) Kinetics of colchicine binding to purified β-tubulin isotypes from bovine brain. *J. Biol. Chem. 267*, 13335–13339.
19. Dumortier, C., Potenziano, J. L., Bane, S., and Engelborghs, Y. (1997) The mechanism of tubulin-colchicine recognition: A kinetic study of the binding of a bicyclic colchicine analogue with a minor modification of the A ring. *Eur. J. Biochem. 249*, 265–269.
20. Banerjee, A., Engelborghs, Y., Luduena, R. F., and Fitzgerald, T. J. (1995) The role of the B-ring of colchicine in its interaction with pure tubulin isoforms α-β(II), α-β(III), and α-β(IV). *Mol. Biol. Cell 6*, 173.
21. Xu, K., Schwarz, P. M., and Luduena, R. F. (2002) Interaction of nocodazole with tubulin isotypes. *Drug Dev. Res. 55*, 91–96.
22. Murphy, D. B., Wallis, K. T., Machlin, P. S., Ratrie, H., and Cleveland, D. W. (1987) The sequence and expression of the divergent β-tubulin in chicken erythrocytes. *J. Biol. Chem. 262*, 14305–14312.
23. Joshi, H. C., Yen, T. J., and Cleveland, D. W. (1987) In vivo coassembly of a divergent β-tubulin subunit (C-β6) into microtubules of different function. *J. Cell Biol. 105*, 2179–2190.
24. Schwer, H. D., Lecine, P., Tiwari, S., Italiano, J. E., Hartwig, J. H., and Shivdasani, R. A. (2001) A lineage-restricted and divergent

β-tubulin isoform is essential for the biogenesis, structure and function of blood platelets. *Curr. Biol. 11*, 579–586.
25. Murphy, D. B., and Wallis, K. T. (1985) Erythrocyte microtubule assembly in vitro: Determination of the effects of erythrocyte-tau, tubulin isoforms, and tubulin oligomers on erythrocyte tubulin assembly, and comparison with brain microtubule assembly. *J. Biol. Chem. 260*, 2293–2301.
26. Murphy, D. B., and Wallis, K. T. (1983) Isolation of microtubule protein from chicken erythrocytes and determination of the critical concentration for tubulin polymerization in vitro and in vivo. *J. Biol. Chem. 258*, 8357–8364.
27. Murphy, D. B., and Wallis, K. T. (1986) Erythrocyte microtubule assembly in vitro: Tubulin oligomers limit the rate of microtubule self-assembly. *J. Biol. Chem. 261*, 2319–2324.
28. Trinczek, B., Marx, A., Mandelkow, E. M., Murphy, D. B., and Mandelkow, E. (1993) Dynamics of microtubules from erythrocyte marginal bands. *Mol. Biol. Cell 4*, 323–335.
29. Staretz, M. E., and Hastie, S. B. (1993) Synthesis and tubulin binding of novel C-10 analogs of colchicine. *J. Med. Chem. 36*, 758–764.
30. Chabin, R. M., and Hastie, S. B. (1989) Association of thiocolchicine with tubulin. *Biochem. Biophys. Res. Commun. 161*, 544–550.
31. Sharma, S., Ganesh, T., Kingston, D. G. I., and Bane, S. (2007) Promotion of tubulin assembly by poorly soluble taxol analogs. *Anal. Biochem. 360*, 56–62.
32. Williams, R. C., and Lee, J. C. (1982) Purification of tubulin from brain. *Methods Enzymol. 85*, 376–385.
33. Sackett, D. L. (1995) Rapid purification of tubulin from tissue and tissue-culture cells using solid-phase ion-exchange. *Anal. Biochem. 228*, 343–348.
34. Penefsky, H. S. (1979) Preparation of nucleotide-depleted F1 and binding of adenine nucleotides and analogs to the depleted enzyme. *Methods Enzymol. 55*, 377–380.
35. Detrich, H. W., and Williams, R. C. (1978) Reversible dissociation of the α-β dimer of tubulin from bovine brain. *Biochemistry 17*, 3900–3907.
36. Hastie, S. B. (1989) Spectroscopic and kinetic features of allocolchicine binding to tubulin. *Biochemistry 28*, 7753–7760.
37. Pyles, E. A., and Hastie, S. B. (1993) Effect of the B-ring and the C-7 substituent on the kinetics of colchicinoid tubulin associations. *Biochemistry 32*, 2329–2336.
38. Lakowicz, J. R. (1999) Principles of Fluorescence Spectroscopy, 2nd ed., Kluwer Academic/Plenum Publishers, New York.
39. Medrano, F. J., Andreu, J. M., Gorbunoff, M. J., and Timasheff, S. N. (1989) Roles of colchicine ring-B and ring-C in the binding process to tubulin. *Biochemistry 28*, 5589–5599.
40. Ravelli, R. B. G., Gigant, B., Curmi, P. A., Jourdain, I., Lachkar, S., Sobel, A., and Knossow, M. (2004) Insight into tubulin regulation from a complex with colchicine and a stathmin-like domain. *Nature 428*, 198–202.
41. Huzil, J. T., Luduena, R. F., and Tuszynski, J. (2006) Comparative modelling of human β tubulin isotypes and implications for drug binding. *Nanotechnology 17*, S90–S100.
42. Bhattacharyya, B., and Wolff, J. (1984) Immobilization-dependent fluorescence of colchicine. *J. Biol. Chem. 259*, 1836–1843.
43. Skoufias, D. A., and Wilson, L. (1992) Mechanism of inhibition of microtubule polymerization by colchicine: Inhibitory potencies of unliganded colchicine and tubulin colchicine complexes. *Biochemistry 31*, 738–746.
44. Schonbrunn, E., Phlippen, W., Trinczek, B., Sack, S., Eschenburg, S., Mandelkow, E. M., and Mandelkow, E. (1999) Crystallization of a macromolecular ring assembly of tubulin liganded with the antimitotic drug podophyllotoxin. *J. Struct. Biol. 128*, 211–215.
45. Friedman, P. A., and Platzer, E. G. (1978) Interaction of anthelmintic benzimidazoles and benzimidazole derivatives with bovine brain tubulin. *Biochim. Biophys. Acta 544*, 604–614.
46. Dumortier, C., Gorbunoff, M. J., Andreu, J. M., and Engelborghs, Y. (1996) Alterations of rings B and C of colchicine are cumulative in overall binding to tubulin but modify each kinetic step. *Biochemistry 35*, 15900–15906.
47. Cortese, F., Bhattacharyya, B., and Wolff, J. (1977) Podophyllotoxin as a probe for the colchicine binding site of tubulin. *J. Biol. Chem. 252*, 1134–1140.
48. Banerjee, A., Roach, M. C., Trcka, P., and Luduena, R. F. (1990) Increased microtubule assembly in bovine brain tubulin lacking the type-III isotype of β-tubulin. *J. Biol. Chem. 265*, 1794–1799.
49. Khan, I. A., Tomita, I., Mizuhashi, F., and Luduena, R. F. (2000) Differential interaction of tubulin isotypes with the antimitotic compound IKP-104. *Biochemistry 39*, 9001–9009.
50. Chaudhuri, A. R., Seetharamalu, P., Schwarz, P. M., Hausheer, F. H., and Luduena, R. F. (2000) The interaction of the B-ring of colchicine with α-tubulin: A novel footprinting approach. *J. Mol. Biol. 303*, 679–692.
51. Joe, P. A., Banerjee, A., and Luduena, R. F. (2008) The roles of Cys124 and Ser239 in the functional properties of human βIII tubulin. *Cell Motil. Cytoskeleton 65*, 476–486.
52. Andreu, J. M., Perez-Ramirez, B., Gorbunoff, M. J., Ayala, D., and Timasheff, S. N. (1998) Role of the colchicine ring A and its methoxy groups in the binding to tubulin and microtubule inhibition. *Biochemistry 37*, 8356–8368.
53. Wang, D., Villasante, A., Lewis, S. A., and Cowan, N. J. (1986) The mammalian β-tubulin repertoire: Hematopoietic expression of a novel, heterologous β-tubulin isotype. *J. Cell Biol. 103*, 1903–1910.
54. Lewis, S. A., Gu, W., and Cowan, N. J. (1987) Free intermingling of mammalian β-tubulin isotypes among functionally distinct microtubules. *Cell 49*, 539–548.
55. Zhou, J., and Giannakakou, P. (2005) Targeting microtubules for cancer chemotherapy. *Curr. Med. Chem.: Anti-Cancer Agents 5*, 65–71.
56. Hartmann, J. T., and Lipp, H. P. (2006) Camptothecin and podophyllotoxin derivatives: Inhibitors of topoisomerase I and II: Mechanisms of action, pharmacokinetics and toxicity profile. *Drug Saf. 29*, 209–230.
57. Escuin, D., Burke, P. A., McMahon-Tobin, G., Hembrough, T., Wang, Y. F., Alcaraz, A. A., Leandro-Garcia, L. J., Rodriguez-Antona, C., Snyder, J. P., LaVallee, T. M., and Giannakakou, P. (2009) The hematopoietic-specific β1-tubulin is naturally resistant to 2-methoxyestradiol and protects patients from drug-induced myelosuppression. *Cell Cycle 8*, 3914–3924.